Thermopower and resistivity of amorphous and crystalline NiP

P. J. Cote and L. V. Meisel
United States Army Armament Research and Development Command, Benet Weapons Laboratory, Watervliet Arsenal, Watervliet, New York 12189
(Received 18 June 1979)

Data are presented for the thermopower and electrical resistivity of amorphous and crystalline $Ni_{76}P_{24}$. Mean-free-path effects are large in the electrical resistivity but appear to be less significant in the thermopower. The diffraction model, modified to include the Pippard-Ziman constraint on the electron-phonon interaction, is used to derive an expression for the thermopower in high-resistivity systems. The data on the amorphous phase are consistent with this modified diffraction model. The *s-d* model predictions, in contrast, are an order of magnitude too large and of the wrong sign.

I. INTRODUCTION

The diffraction model of electrical transport is well established for ideal crystalline metals (Bloch-Grüneisen function[1]) and for liquid metals [Ziman theory[2] and its extension to transition metals by Evans, Greenwood, and Lloyd (EGL)[3,4]]. The model has also been adapted to the study of electrical transport in crystalline,[5] amorphous,[6-11] and disordered alloys,[6-11] and good agreement has been obtained for the temperature dependences and magnitudes of the measured resistivity ρ and thermopower Q in many systems. However, significant discrepancies are found between theory and experiments in high-resistivity alloys ($\rho > 150\ \mu\Omega$ cm).[12] For example, (assuming backscattering dominant and a Debye phonon spectrum) the diffraction model gives $\rho \propto 1 + AT^2$, with A a positive constant for temperatures T much less than the Debye temperature Θ in all amorphous metals, while systems with $\rho > 150\ \mu\Omega$ cm generally exhibit $\rho \propto 1 - AT^2$. We have shown[13] that such discrepancies can be understood in the framework of the diffraction model by incorporating the Pippard-Ziman mean-free-path condition on the electron-phonon interaction.[14] (The effect of the Pippard-Ziman condition is to reduce the inelastic part of the resistivity at the highest resistivities.)

Electrodeposited NiP alloys are well characterized and thus are excellent subjects for examining theoretical models of transport in transition-metal systems. Their heat capacity,[15] x-ray[16] and optical[17] photoemission spectra, electrical resistivity,[18] and magnetic properties[19] have been studied. In addition, amorphous NiP alloys transform into several crystalline phases of varying residual resistivity. The extensive range of magnitudes and temperature dependences of resistivity and thermopower exhibited by these alloys subjects any transport theory to stringent tests.

The electrical resistivity data reported here indicate that strong mean-free-path effects are present and are well described by the modification of the diffraction model given in Ref. 13. Thermopower, on the other hand, is not as sensitive to electron mean-free-path effects since it is determined primarily by elastic scattering in these highly disordered systems. The present thermopower results are in good agreement with the diffraction model. On the other hand, the s-d scattering model[20,21] (the principal alternative theory in transition-metal systems) predicts the wrong sign and magnitude for the thermopower of these alloys.

II. THEORY

The diffraction model (extended Ziman theory[3]) gives

$$\rho = \frac{24\pi^3}{\Omega_0 k_F^2 E_F} \sum_{i,j,l,m} \alpha_{lm}^{ij} I_{lm}^{ij}, \tag{1}$$

where all quantities are in atomic units (atomic unit of resistivity is $\hbar/\mathrm{Ry} = 43.48\ \mu\Omega$ cm), Ω_0 is the atomic volume, k_F is the Fermi wave number, E_F is the Fermi energy,

$$\alpha_{lm}^{ij} \equiv (2l+1)(2m+1)\sin\eta_l^i \sin\eta_m^j e^{i(\eta_l^i - \eta_m^j)}, \tag{2}$$

where η_l^i is the lth scattering phase shift evaluated at the Fermi energy on the ith component of the alloy, and

$$I_{lm}^{ij} \equiv (c_i c_j)^{1/2} \int_0^1 dx\, x^3 S_{ij}(2k_F x) F_{lm}(x), \tag{3}$$

where c_i is the concentration of the ith component, S_{ij} is the partial structure factor, and

$$F_{lm}(x) = P_l(1-2x^2) P_m(1-2x^2),$$

with P_l the lth Legendre polynomial.

The thermopower Q is given as (dropping component indices)

$$Q = (\pi^2 k_B T/3|e|E_F)(-\xi), \tag{4}$$

where

$$-\xi \equiv \tfrac{1}{2}\frac{\partial(\ln\rho)}{\partial(\ln k_F)} = -2 + y + z \,, \tag{5}$$

with

$$y = \tfrac{1}{2}k_F \sum \alpha_{lm} \frac{\partial I_{lm}}{\partial k_F} \Big/ \sum \alpha_{lm} I_{lm} \tag{6}$$

and

$$z = \tfrac{1}{2}k_F \sum \frac{\partial \alpha_{lm}}{\partial k_F} I_{lm} \Big/ \sum \alpha_{lm} I_{lm} \tag{7}$$

(k_B is Boltzmann's constant, e is the electron charge, and T is the absolute temperature). The d-phase shift term and backscattering dominate the electrical transport properties of transition-metal (TM) alloys; thus

$$\rho \approx (30\pi^3/\Omega_0 k_F E_F) c_{TM} \sin^2(\eta_2^{TM}) S_{TM}(2k_F) \,, \tag{8}$$

$$y \approx \tfrac{1}{2} \frac{\partial(\ln S_{TM})}{\partial(\ln k_F)} \,, \tag{9}$$

and

$$z \approx k_F \cot(\eta_2^{TM}) \frac{\partial \eta_2^{TM}}{\partial k_F} \,. \tag{10}$$

The temperature and composition dependence of the electrical resistivity in amorphous and disordered crystalline alloys is essentially determined by the (resistivity) partial structure factors. The thermopower is determined by derivatives of the phase shifts and structure factors as well.

The x-ray and resistivity structure factors for amorphous Debye solids are discussed in Refs. 7 and 8. There is an extensive literature dealing with the structure factors of liquid metals. The (resistivity) partial structure factors can be separated into elastic and inelastic components. Employing the Sham-Ziman approximation[22] to the multiphonon series, one obtains

$$S(K) = S_0(K) + S_{ph}(K) \,, \tag{11}$$

where the elastic component

$$S_0(K) = a(K)\, e^{-2W(K)} \,, \tag{12}$$

with $a(K)$ being the geometric structure factor and $e^{-2W(K)}$ the Debye-Waller factor; the phonon (or inelastic) component for a Debye phonon spectrum is given by

$$S_{ph}(K) = \alpha(K)(\Theta/T) \times \int_\gamma^1 \left(\frac{q}{q_D}\right)^2 d\left(\frac{q}{q_D}\right) n(x)[n(x)+1] \times \int \frac{d\Omega}{4\pi} a(|\vec{K}+\vec{q}|) \,, \tag{13}$$

where $\alpha(K) \equiv 3(\hbar K)^2/Mk_B\Theta$, M is the average ionic mass, q_D and Θ the Debye wave number and temperature, $n(x) \equiv (e^x - 1)^{-1}$ is the phonon occupation number, and $x = \hbar\omega/k_BT = (q/q_D)(\Theta/T)$ for a Debye phonon spectrum. The lower limit γ is determined by the electron mean free path through the Pippard-Ziman condition[13,14] and is defined below. If the resistivity is not too large, the entire phonon spectrum contributes, and $\gamma = 0$. In that case $S \propto 1 + AT^2$, with A a positive constant at low temperatures ($T \ll \Theta$) since the coefficient of the $+T^2$ term in the inelastic term is approximately twice as large as the $-T^2$ term in the elastic term (arising from the Debye-Waller factor). We note here that the T^5 contribution to ρ, arising from the $K = 0$ singularity in $a(K)$[11] is negligible because of the large weighting of $K \approx 2k_F$ scattering in TM systems, and has never been observed.

The high electrical resistivity of amorphous metals indicates that the electron mean free path is short. In such cases the Pippard-Ziman condition[14] on the electron-phonon interaction must be considered. Following Ziman, this condition may be expressed as follows: *phonons with wavelengths longer than the electron mean free path* Λ *are ineffective electron scatterers*. The low frequency cutoff at $q/q_D = \gamma$ in Eq. (13) is a direct consequence of this condition. The factor γ can be related to the resistivity ρ as $\gamma = \rho/\rho^*$, with the saturation resistivity

$$\rho^* \equiv 3q_D/2\pi N(E_F) e^2 V_F \,, \tag{14}$$

where $N(E_F)$ is the density of conduction states at the Fermi energy and V_F is the Fermi velocity. For free-electron metals, $\rho^* \sim 200 - 300\ \mu\Omega\,\text{cm}$. Expressing the resistivity partial structure factors as explicit functions of γ, one has for $T \gtrsim \frac{1}{2}\Theta$ and $\gamma < 1$,

$$S(K,\gamma) \cong a(K) e^{-2W(K)} + (1-\gamma) S_{ph}(K,0) \,. \tag{15}$$

Thus

$$\rho = \rho_0 e^{-2\bar{W}} + (1 - \rho/\rho^*)\rho_{ip} = \frac{\rho_0 e^{-2\bar{W}} + \rho_{ip}}{1 + \rho_{ip}/\rho^*} \,, \tag{16}$$

where ρ_{ip} is the ideal-phonon resistivity (which is approximately linear in T for $T > \frac{1}{2}\Theta$) and $\rho_0 e^{-2\bar{W}}$ is

the elastic component of the resistivity. [$2\bar{W} \approx 2W(2k_F)$ is an effective Debye-Waller exponent.] This expression is expected to apply to crystalline metals as well.[13]

Equation (16) reproduces the observations of Mooij[12] concerning saturation effects. For example, for $\rho_0 \approx 0$, ρ becomes approximately T independent as $\rho_{ip} \to \rho^*$; and for $\rho_0 > \frac{1}{2}\rho^*$, negative temperature coefficients of resistivity (TCR) occur because of the dominance of the elastic contributions to the resistivity for $\gamma > \frac{1}{2}$, regardless of the position of $2k_F$ with respect to the first peak in the structure factor.

The denominator in Eq. (16) will give rise to extra terms in the thermoelectric parameter:

$$-\xi = -2 + y + z - \frac{\rho_{ip}}{\rho^* + \rho_{ip}}\left[-2 + y^* + z^* + \left(\frac{1}{2} + \frac{\partial \ln(N(E_F))}{\partial \ln E_F}\right)\right] \tag{17}$$

where y and z are defined in Eqs. (6) and (7) and

$$y^* = \tfrac{1}{2}k_F \sum \alpha_{lm} \frac{\partial J_{lm}}{\partial k_F} \Big/ \sum \alpha_{lm} J_{lm}, \tag{18}$$

$$z^* = \tfrac{1}{2}k_F \sum \frac{\partial \alpha_{lm}}{\partial k_F} J_{lm} \Big/ \sum \alpha_{lm} J_{lm}, \tag{19}$$

and

$$J_{lm}^{ij} = (c_i c_j)^{1/2} \int dx\, x^3 S_{ij}^{ph}(2k_F x) F_{lm}(x). \tag{20}$$

We have dropped the i,j superscripts in Eqs. (18) and (19) as before, and $S_{ij}^{ph}(K)$ is the ideal-phonon part of the ijth partial-structure factor. Consider two special cases:

(i) Ideal-phonon resistivity is much less than saturation resistivity ($\rho_{ip} \ll \rho^*$). The new terms are small in this limit and Eq. (15) is recovered. Thus, as long as $\rho_{ip} \ll \rho^*$, Eq. (5) is a good approximation to the thermopower, even in cases in which saturation effects, generated by elastic scattering (i. e., $\rho_0 \approx \rho^*$), are important in determining the TCR.

(ii) Elastic scattering contributions are much less than phonon scattering contributions to the resistivity ($\rho_0 e^{-2\bar{W}} \ll \rho_{ip}$). In this limit $I_{lm}^{ij} = J_{lm}^{ij}$, so that $y = y^*$ and $z = z^*$, and

$$-\xi = \frac{1}{1 + \rho_{ip}/\rho^*}(-2 + y + z) - \frac{\rho_{ip}}{\rho^* + \rho_{ip}}\left(\frac{1}{2} + \frac{\partial \ln N(E_F)}{\partial \ln E_F}\right). \tag{21}$$

We see that in this limit, appropriate to perfect-crystalline materials, the thermoelectric parameter is reduced by the same factor, $1 + \rho_{ip}/\rho^*$, as is the resistivity, and there is an additional correction term. In the limit of very large ρ_{ip}, $-\xi$ goes to -1 for a free-electron density of states, which is the standard result in the constant mean-free-path case.[23]

III. EXPERIMENTAL DETAILS

Amorphous NiP samples were produced by electrodeposition using bath conditions established by Brenner *et al.*[24] The composition of the samples was determined by wet chemistry techniques. The Ni concentration of all samples was approximately 74 at.%. Resistivity and thermopower were measured simultaneously using the four-probe arrangement described by Middleton and Scanlon.[25] Copper-Constantan thermocouples were spot welded to the ends of the sample. A Leeds and Northrup five-dial potentiometer was employed in the resistivity determinations and a Keithley microvoltmeter was used in the thermopower measurements.

IV. RESULTS

Resistivity ρ vs temperature T for amorphous and crystalline phases is plotted in Fig. 1. The amorphous phase exhibits a small positive TCR, in agreement with earlier results[18] which indicate a crossover from positive to negative TCR near 74-at.% Ni composition.

Raising the temperature beyond 500 K led to a rapid reduction in resistivity on crystallization to the disordered Ni_xP_y + Ni phase recently reported by Vafaei-Makshoos *et al.*[26] Heating beyond 600 K yields a transformation to the stable Ni_3P + Ni

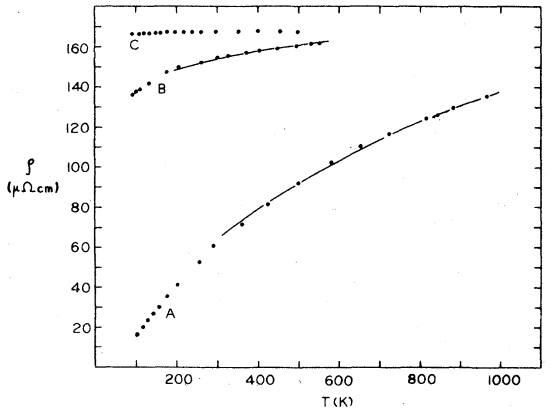

FIG. 1. Electrical resistivity of amorphous and crystalline NiP. Curve A: crystalline Ni_3P (+Ni). Curve B: disordered crystalline Ni_xP_y (+Ni). Curve C: amorphous $Ni_{76}P_{24}$. The solid lines are fits to the data using Eq. (16); the fitting parameters are given in the text.

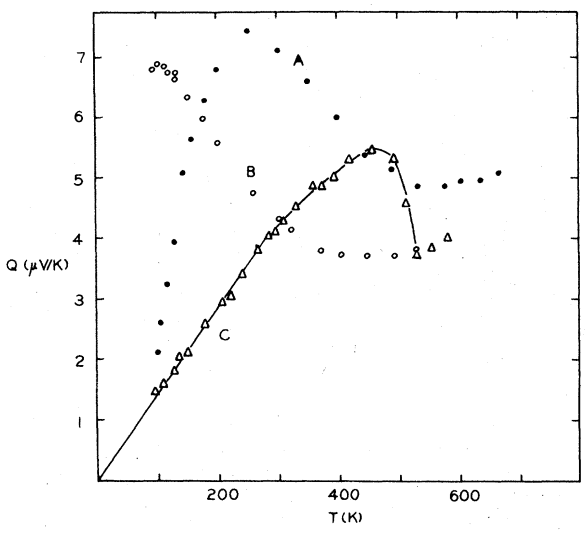

FIG. 2. Thermoelectric power of amorphous and crystalline NiP. Curve A: crystalline Ni_3P (+Ni). Curve B: disordered crystalline Ni_xP_y (+Ni). Curve C: amorphous $Ni_{76}P_{24}$. The rapid drop in Q beyond 450 °C is due to crystallization to the disordered Ni_xP_y phase.

phase and a corresponding large reduction in resistivity. (The small residual resistivity for Ni_3P is expected for compound formation.) These crystallization processes, seen in the resistivity, have been characterized by calorimetry,[27] x-ray diffraction,[27] electron diffraction and microscopy,[26] and x-ray[16] and optical-absorption[17] studies. The resistivity of amorphous and crystalline $Ni_{80}P_{20}$ between 4.2 and 300K has also been reported.[18]

Thermopower Q vs temperature T for the amorphous and crystalline phases is plotted in Fig. 2. The thermopower of the amorphous phase is linear in temperature over most of the range, with a small negative deviation from linearity appearing above room temperature. (Identical results were obtained in two other samples of similar composition.)

Dramatic differences between the thermopower results of the amorphous and crystalline phases are evident. There is a 35% reduction in the thermopwer on crystallization to the Ni_xP_y + Ni phase, while the resistivity decreases by only 5%; and the large peaks seen near 100 K in Ni_xP_y + Ni and near 250 K in Ni_3P + Ni are not seen in the amorphous phase. If one assumes that the peaks represent extra contributions beyond the diffusion component of the thermopower Q_d, then the overall trends suggest that Q_d is linear in T with $Q_d/T \approx 0.007\ \mu VK^{-2}$ in the crystalline phases. This may be compared with $Q/T \approx 0.013\ \mu VK^{-2}$ in the amorphous phase.

V. DISCUSSION

A. Electrical resistivity

1. Crystalline phases

Curve A in Fig. 1 shows ρ vs T for Ni_3P. The residual resistivity is small and the resistivity increases rapidly with temperature below 300 K. Above 300 K a large negative deviation from linearity is evident, indicating a major loss of temperature dependence for ρ. The solid line obtained using $\rho^* = 290\ \mu\Omega$cm, $\rho_{ip} = 0.27\ T\ \mu\Omega$cm K^{-1}, and $\rho_0 = 0$ in Eq. (16) fits the high-temperature ($T \gtrsim \Theta$) data well. [At lower temperatures $\gamma (= \rho/\rho^*)$ is small so that agreement between standard theory and experiment is expected.]

Curve B of Fig. 1 shows ρ vs T in the disordered Ni_xP_y + Ni phase. The residual resistivity is large and the temperature dependence of ρ is much smaller than that of the Ni_3P phase over the entire range of temperatures. The solid line was obtained from Eq. (16) using $\rho^* = 245\ \mu\Omega$cm, $\rho_{ip} = 0.29T\ \mu\Omega$cm K^{-1}, $\rho_0 = 130\ \mu\Omega$cm, and effective Debye-Waller exponent $2\tilde{W} = T/100$ K. The saturation resistivity ρ^* and ideal-phonon resistivity ρ_{ip} deduced from the two crystalline phases are consistent, the residual resistivity is determined from the data, and the effective Debye-Waller exponent is reasonable for a system in which backscattering is dominant and the electron per atom ratio is unity.

These results are examples of the universal trend discovered by Mooij[12] that the temperature dependence of the resistivity of metals is lost as ρ approaches 200 $\mu\Omega$cm, whether the origin of ρ is electron-phonon scattering or disorder. The usual explanation is that, as ρ approaches 200 $\mu\Omega$cm, the electron mean free path approaches an interatomic spacing so that additional thermal disorder cannot further reduce the mean free path. This is consistent with the ideas used to derive Eq. (16)

2. Amorphous phase

Curve C of Fig. 1 shows ρ vs T for amorphous NiP. The residual resistivity is higher than that of the disordered crystalline phase, and the TCR is smaller, suggesting that these results are another example of the Mooij trend (i.e., mean-free-path or saturation effects). However, the amorphous metal case is less clear since the standard diffraction model predicts small TCR values for amorphous metals. Nevertheless, careful analysis of the temperature dependence of ρ in high-resistivity amorphous metals shows that mean-free-path effects are important, particularly at low temperatures where the standard diffraction mo-

del always predicts positive TCR while the highest resistivity ($\rho_0 \gtrsim \frac{1}{2}\rho^*$) amorphous and disordered crystalline metals exhibit negative TCR.

B. Thermoelectric power

The thermoelectric power data are shown in Fig. 2. The discussion will center on the thermopower of amorphous NiP (curve C) and its implications for transport theory. The crystalline thermopower (curves A and B) will be considered briefly at the end of this section. The principal result for the amorphous phase is that the thermoelectric power Q is linear in T with a slope $Q/T = +0.013\ \mu V K^{-2}$. We shall compare this result with the predictions of the diffraction model and with the principal alternative for transition-metal systems, Mott's s-d model.[20,21] Many authors prefer the s-d model in transition-metal systems; for example, Enderby and Dupree[21] have taken this position because of difficulties encountered in explaining the thermopower of liquid iron with the diffraction model.

First we discuss the diffraction model predictions of the thermopower. For glassy NiP it is found[8] that the ideal-phonon resistivity ρ_{id} was small compared with ρ, which is less than ρ^*. If we assume that the dominant terms are given by the $l=2$ phase shift in Ni, we can use Eq. (5) and the approximate Eqs. (8)–(10). The scattering phase-shift contribution to $(-\xi)$ of Eq. (5) is given by $z=-4.4$. Thus the structural contribution y must be positive and larger than 6.4 to explain the positive thermopower in amorphous NiP. This will occur if the Fermi sphere diameter $2k_F$ corresponds to the rapidly increasing portion of the main peak of the Ni-Ni partial structure factor, which is exactly the same condition required to explain the temperature and composition dependence of the electrical resistivity of amorphous NiP. One obtains $Q/T \approx +0.006\ \mu V K^{-2}$ using the values of $S_{\mathrm{Ni\text{-}Ni}}(K)$ measured by Waseda *et al.*[28] (Calculations based upon Percus-Yevick partial structure factors as used in Ref. 6 yield Q/T values in the range from 0.008 to 0.011 $\mu V K^{-2}$.) Considering the crudeness of the approximations incorporated in these computations, the results reflect good agreement with experiment and provide support for the diffraction model description of transport in amorphous transition-metal alloys.

This support appears even stronger if we consider the predictions of the s-d model for NiP. The electronic structure studies indicate that the Fermi energy E_F is in the rapidly decreasing part of the d-band density of states $N_d(E)$. According to the s-d model ρ is proportional to $N_d(E_F)$ and so the thermoelectric power is proportional to

$$\left(\frac{\partial \ln \rho}{\partial E}\right)_{E_F} \approx \left(\frac{\partial \ln N_d(E)}{\partial E}\right)_{E_F}.$$

From the x-ray photoemission (XPS) results[16] on amorphous NiP an optimistic estimate of Q/T would be $-0.3\ \mu V K^{-2}$, which is an order of magnitude too large and has the wrong sign. Similar discrepancies between the s-d model predictions and measured thermopower in amorphous BeZrTi were reported by Nagel.[29]

The liquid Ni case is related to the question of the thermopower of the noncrystalline NiP system. The initial agreement[3] of the predictions of the EGL theory with the thermopower of liquid Ni (see Ref. 21) was based on the choice of 2 for the electron to atom ratio, which places $2k_F$ to the right of the first peak in the structure factor and gives a negative value for y in Eq. (5). Later results suggest that the appropriate electron to atom ratio is closer to 1, which places $2k_F$ to the left of the peak in the structure factor and yields a positive value for y. We therefore expect this to adversely affect the agreement with experiment, and, in fact, a subsequent calculation,[30] using 1 for the electron to atom ratio gave $Q=-12\ \mu V K^{-1}$ vs $-38\ \mu V K^{-1}$ for the measured value[21] for liquid Ni at 1489°C. Although the sign difference between the thermopower of amorphous NiP and liquid Ni is consistent with the diffraction model, serious questions remain regarding the calculated value for Q in liquid Ni. Mott[20] has suggested, for example, that the EGL model may be inadequate for pure transition elements.

Because of the high resistivity of amorphous NiP, saturation effects may be present in Q. We have assumed that NiP corresponds to the case presented in the theory section in which $\rho_{id} \ll \rho^*$ and elastic scattering is dominant; however, a negative deviation from linearity is seen in the data for Q at high temperatures, suggesting that ρ_{id} is large enough to generate a significant negative contribution to Q [Eq. (17)].

The thermopower data for the crystalline phases are shown in curves A and B of Fig. 2. Large peaks are seen below room temperature, in striking contrast to the results in the amorphous phase. In particular, although the resistivities of the disordered Ni_xP_y + Ni phase and the amorphous phase are quite similar (large ρ_0, small TCR), there is a large difference between the thermopower data. Since the electronic structure (as determined by XPS) appears to be essentially the same in these phases this may be a result of the differences inherent between amorphous and crystalline structures. Magnetic effects cannot be ruled out, however, until the magnetic properties of the crystalline phases are better established at these compo-

sitions.

In conclusion, the diffraction model provides a consistent picture of the transport properties of amorphous NiP alloys. It is clearly superior to the *s-d* model in this system, although there is evidence of breakdown in the diffraction model at the highest resistivities. Incorporation of mean-free-path effects (through the Pippard-Ziman condition) into the diffraction model yields good agreement with transport properties at the highest resistivities in amorphous and disordered crystalline NiP alloys; related mean-free-path effects are seen in thermal conductivity[31] and ultrasonic attenuation.[32]

---

[1]A. H. Wilson, *Theory of Metals* (Cambridge University, Cambridge, England, 1958).

[2]J. M. Ziman, Philos. Mag. 6, 1013 (1961).

[3]R. Evans, D. A. Greenwood, and P. Lloyd, Phys. Lett. A 35, 57 (1971).

[4]O. Dreirach, R. Evans, H. -J. Guntherodt, and H. V. Kunzi, J. Phys. F 2, 709 (1972).

[5]S. N. Khanna and Ashok Jain, J. Phys. F 7, 2523 (1977).

[6]L. V. Meisel and P. J. Cote, Phys. Rev. B 15, 2970 (1977).

[7]P. J. Cote and L. V. Meisel, Phys. Rev. Lett. 39, 102 (1977).

[8]L. V. Meisel and P. J. Cote, Phys. Rev. B 16, 2978 (1977); 17, 4652 (1978).

[9]S. R. Nagel, Phys. Rev. B 16, 1694 (1977).

[10]Y. Waseda and H. S. Chen, Phys. Status Solidi B 87, 777 (1978).

[11]K. Froböse and J. Jäckle, J. Phys. F 1, 2331 (1977).

[12]J. H. Mooij, Phys. Status Solidi A 17, 521 (1973).

[13]P. J. Cote and L. V. Meisel, Phys. Rev. Lett. 40, 1586 (1978).

[14]J. M. Ziman, *Electrons and Phonons* (Clarendon, Oxford, 1960), Chap. V.

[15]Y. S. Tyan and L. E. Toth, J. Electron. Mater. 3, 791 (1974).

[16]K. Suzuki, F. Itoh, T. Fukunaga, and T. Honda, *Rapidly Quenched Metals III, Proceedings of the Third International Conference, Brighton, England, 1978*, edited by B. Cantor (The Metals Society, London, 1978), Vol. 2, p. 410.

[17]J. Rivary and B. Bouchet, in Ref. 16. p. 56 Vol. 2.

[18]P. J. Cote, Solid State Commun. 18, 1311 (1976).

[19]D. Pan and D. Turnbull, AIP Conf. Proc. 18, 646 (1973); A. Berrada, M. F. Lapierre, B. Loegel, P. Panissod, and C. Robert, J. Phys. F 8, 845 (1978).

[20]N. F. Mott, Philos. Mag. 26, 1249 (1972); F. Brouers and M. Brauwers, Z. Phys. 36, L17 (1975).

[21]J. E. Enderby and B. C. Dupree, Philos. Mag. 35, 791 (1977).

[22]L. J. Sham and J. M. Ziman, Solid State Phys. 15, 221 (1961).

[23]R. D. Barnard, *Thermoelectricity in Metals and Alloys* (Wiley, New York, 1972), Chap. 3.

[24]A. Brenner, D. E. Couch, and E. K. Williams, J. Res. Natl. Bur. Stand. 44, 109 (1950).

[25]A. E. Middleton and W. W. Scanlon, Phys. Rev. 92, 219 (1953).

[26]E. Vafaei-Makshoos, E. L. Thomas, and L. E. Toth, Metall. Trans. 9A, 1449 (1978).

[27]B. G. Bagley and D. Turnbull, J. Appl. Phys. 39, 5681 (1968).

[28]Y. Waseda, H. Okazaki, and T. Masumoto, J. Mater. Sci. 12, 1927 (1977).

[29]S. R. Nagel, Phys. Rev. Lett. 41, 990 (1978).

[30]R. Evans, B. L. Gyorffy, N. Szabo, and J. M. Ziman, in *Proceedings of the Second International Conference on Liquid Metals, Tokyo, 1972*, edited by Sakae Takeuchi (Wiley, New York, 1973).

[31]P. G. Klemens, Solid State Phys. 7, 1 (1958); J. E. Zimmerman, J. Phys. Chem. Solids 11, 299 (1959).

[32]A. B. Pippard, Philos. Mag. 46, 1104 (1955); J. Phys. Chem. Solids 3, 175 (1957).